International Journal of Architectural, Civil and Construction Sciences
ISSN: 2415-1734
Vol:6, No:11, 2012

Numerical Investigation on Damage Evolution of Piles inside Liquefied Soil Foundation - *Dynamic-Loading Experiments* -

Ahmed Mohammed Youssef Mohammed, Mohammad Reza Okhovat, and Koichi Maekawa

***Abstract*—**The large and small-scale shaking table tests, which was conducted for investigating damage evolution of piles inside liquefied soil, are numerically simulated and experimental verified by the3D nonlinear finite element analysis. Damage evolution of elasto-plastic circular steel piles and reinforced concrete (RC) one with cracking and yield of reinforcement are focused on, and the failure patterns and residual damages are captured by the proposed constitutive models. The superstructure excitation behind quay wall is reproduced as well.

***Keywords*—**Soil-Structure Interaction, Piles, Soil Liquefaction.

I. Introduction

IN NiigataEarthquake1964, the remarkable damages caused by soil liquefaction to on- and underground structures were reported [1].After Niigata and Alaska Earthquakes (1964), a great attention has been paid to seismic performances of pile-foundation and raised up after the severe damage caused by Hyogoken-Nanbu Earthquake (1995 in Kobe).

The detailed investigation of the instances of remarkable damage has led to further understanding of failure modes and the ultimate limit states, shedding light on aspects such as land sliding, ground liquefaction, soil-structure interaction and the ductility of RC and pile structural elements. Series of variant scale experiments under both static and dynamic loads have been carried out to gain a better understanding of the damage evolution of both piles and soil foundations [2, 3 and 4].

Although earthquakes cannot be prevented, their impacts can be managed to a large extent so that loss to life and property can be minimized. The authors seek for highly inelastic behavioral simulation for risk assessment, performance based design and seismic strengthening of existing infrastructures in service. The main function of the pile-foundation is to act as an axially compressed member in static cases. When earthquake comes and sever liquefaction of soil occurs the pile would be under load combination of flexure, shear force and varying axial compression-tension. To this end, the experimental verification is thought to be indispensable for a reliable simulation where structural and constituent material's damages may be reproduced correctly. In fact, steel and/or RC piles were within the elastic range in the past many structure-soil interaction tests. Then, the highly inelastic responses of structural members have to be focused on in line with gigantic earthquake problems.

From this point of view, the authors provide computational simulation for two dynamic loading experiments. First, a large-scale test on the group piles with a single sheet pile quay wall subjected to liquefaction induced large ground deformation was targeted (Motamed *et al*2009) [5]. Second, a number of shaking table tests were conducted by Maki *et al*(2004) [6] to evaluate the post-yield response of RC piles embedded in both liquefied and dry soil foundation.

As the stiffness of liquefied soils is much reduced, the magnitude of damage to in-ground piles may be reduced rather than dry soils. But, when large deformation occurs due to the liquefaction, soil stiffness may recover owing to cyclic mobility and underground structural deformation can be largely forced. Under this trade-off, the mode of failure and residual damage of piles are the point of interest. In this study, the damage simulation of piles with soil is carried out by the systematically verified finite element program mainly for RC[7, 8, 9, and 10].

II. Nonlinear Constitutive Models

A. RC Constitutive Model

A reinforced concrete material model was constructed by combining the constitutive laws for cracked concrete and those for reinforcement. The fixed multi-directional smeared crack constitutive equations [7] were used as summarized in Fig. 1. The crack spacing and diameters of reinforcing bars are implicitly taken into account in smeared and joint interface elements no matter how large they are.

The constitutive equations of structural concrete satisfy uniqueness for compression, tension and shear transfer along crack planes. The bond between concrete and reinforcing bars is taken into account in the form of the tension stiffening model, and the space-averaged stress-strain relation of reinforcement is assumed to represent the localized plasticity of steel around concrete cracks. The hysteresis rule of reinforcement is formulated based upon Kato's model [11] for a bare bar under reversed cyclic loads. This RC in-plane constitutive modeling has been verified by member-based and structural-oriented experiments. Herein, the authors skip the details of the RC

Ahmed Mohammed Youssef Mohammed is a Post-Doctoral Researcher, Department of Civil Engineering, The University of Tokyo, Japan (phone: +81-3-5841-7498; fax: +81-3-5841-6010; e-mail: mohammed@concrete.t.u-tokyo.ac.jp).

Mohammad Reza Okhovat holds a PhD degree from Department of Civil Engineering, The University of Tokyo and currently works for Damwatch Services Ltd., Wellington, New Zealand (Phone: +64-4-381-1344; Fax: +64-4-381-1301; E-mail: mohammad.okhovat@damwatch.co.nz).

Koichi Maekawa is Professor, Department of Civil Engineering, The University of Tokyo, Japan (phone: +81-3-5841-7498; fax: +81-3-5841-6010;e-mail: maekawa@concrete.t.u-tokyo.ac.jp).

material modeling by referring to Maekawa *et al.*(2003) [7].

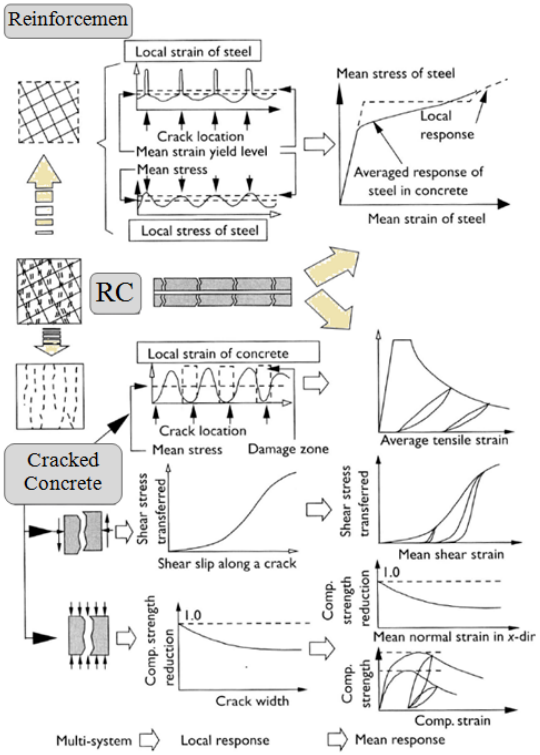

Fig. 1 RC constitutive laws [7]

B. Soil Constitutive Model

A nonlinear path-dependent constitutive model of soil is essential to simulate the entire RC-soil system. Here, the multi-yield surface plasticity concept [7, 8 and 12] is applied to formulate the shear stress-shear strain relation of the soil following Masing's rule [13].

The basic idea of this integral scheme is actualized to sum up component stresses that may represent microscopic events. First, the total stress applied on soil particle assembly, denoted by σ_{ij}, can be decomposed into the deviatoric shear stresses (s_{ij}) and the mean confining stress (p) as,

$$\sigma_{ij} = s_{ij} + p\delta_{ij} \tag{1}$$

where δ_{ij} is Kronecker's delta symbol

Soil is idealized as an assembly of finite numbers of elasto-perfectly plastic components of isotropy, which are conceptually connected in parallel as shown in Fig 2. As each component is given different yield strengths of plasticity which may reflect the grading of the sand particle size, all components subsequently begin to yield at different total shear strains, which results in a gradual increase of entire nonlinearity. The nonlinear behavior appears naturally as a combined response of all components. Hence, the total shear stress carried by soil particles is expressed with regard to an integral of each component stress as,

$$\begin{aligned} s_{ij} &= \sum_{m=1}^{n} s_{ij}^m(\varepsilon_{kl}, \varepsilon_{pkl}^m, G_o{}^m, F^m) \\ ds_{ij}^m &= 2G_o^m de_{eij}^m = 2G_o^m(de_{ij} - de_{pij}^m) \\ de_{pij}^m &= \frac{s_{ij}^m}{2F^m} df, \\ df &= \frac{s_{kl}^m de_{kl}}{F^m} = \frac{s_{kl}^m d\varepsilon_{kl}}{F^m} \end{aligned} \tag{2}$$

where ε_{kl} and ε_{pkl} are the total and plastic strain tensors, respectively, of the (k,l) component, $G_o{}^m$and F^m are the initial shear stiffness and the yield strength, respectively, of the m-th component, and (e_{ij}, $e^m{}_{pij}$, $e^m{}_{eij}$) are the deviatoric tensors of total strain, and those of plastic and elastic strains of the m-th component, respectively. These component parameters can be uniquely decided from the shear stress strain relation of soil under the referential constant confinement [8].

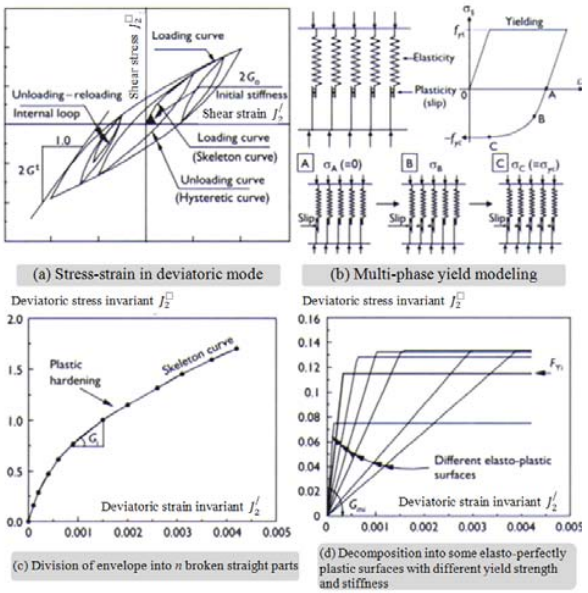

Fig. 2 Constitutive modeling for soil [7]

In general, the volumetric components may fluctuate and affect the shear strength of the soil skeleton under the loading. In reality, the shear strength of soil may decay when increasing pore water pressure leads to reduced confining stress of the soil particle skeleton. The multi-yield surface plastic envelope may inflate or contract according to the confinement stress. It can be formulated by summing up the linear relation of the shear strength and the confinement stress as,

$$\begin{aligned} F^m &= \chi F_{ini}^m \\ \chi &= \frac{(c - I_1' \tan\phi)}{S_u} \\ I_1' &= \frac{(\sigma_1' + \sigma_2' + \sigma_3')}{3} \end{aligned} \tag{3}$$

where S_u is the specific shear strength corresponding to a certain confinement (98kN), F^m_{ini} is the specified yield strength of the m-th component corresponding to the specific S_u, χ is the confinement index, and (c, ϕ) are the cohesive stress and the internal frictional angle, respectively.

For simulation of the pore water pressure and related softening of soil stiffness in shear, the volumetric nonlinearity of the soil skeleton has to be taken into account. The authors simply divided the dilatancy into two components according to the microscopic events. One component is the consolidation (negative dilation) as unrecoverable plasticity denoted by ε_{vc}. The other is the positive dilatancy associated with alternate shear stress due to the overriding of soil particles, which is denoted by ε_{vd} as,

$$p = 3K_0(\varepsilon_0 - \varepsilon_v), \quad \varepsilon_v = \varepsilon_{vc} + \varepsilon_{vd} \tag{4}$$

whereK_0 is the initial volumetric bulk stiffness of soil particles assembly and can be calculated by assuming the initial elastic Poisson's ratio denoted by ν(=0.2) as,

$$K_0 = \frac{2(1+\nu)}{3(1-2\nu)} G_0 \tag{5}$$

The volume reduction of pores among soil particles will cause increasing pore pressure under undrained states, which may lead to liquefaction. According to experiments on sandy soils, the following formulae are adopted.

$$\varepsilon_{vc} = \varepsilon_{v,\lim}\left\{1 - \exp\left(-2(J_{2p} + J_{2p,ini})\right)\right\} - \varepsilon_{vc,ini} \tag{6}$$

$$J_{2p} = \int dJ_{2p}, \quad dJ_{2p} \equiv \frac{1}{2} s_{kl} \cdot d\varepsilon_{kl} \tag{7}$$

whereJ_{2p}represents the accumulated shear strain invariant of the soil skeleton [8 and 14], and $\varepsilon_{v,lim}$ is the intrinsic volumetric compacting strain corresponding to the minimum void ratio as,

$$\begin{aligned} \varepsilon_{vc,ini} &= \varepsilon_{v,\lim}\left\{1 - \exp(-2J_{2p,ini})\right\} \\ \varepsilon_{v,\lim} &= 0.1\left(\log_{10} I_1^{0.6} + 1.0\right) \end{aligned} \tag{8}$$

If the relative density of soil is assumed to be D_r, the following relation can be used to inversely determine $J_{2p,ini}$, which is a constant corresponding to the initial compactness of soil particles as,

$$D_r(\%) = \frac{\varepsilon_{vc,ini}}{\varepsilon_{v,\lim}} = \left\{1 - \exp(-2J_{2p,ini})\right\} \tag{9}$$

The shear provoked dilation, which is path-independent and defined by the updated shear strain intensity J_{2s}, is empirically formulated based on Toyoura sand as,

$$\begin{aligned} \varepsilon_{vd} &= \eta \frac{(a J_{2s})^2}{1 + (a J_{2s})^2} \\ J_{2s} &= \sqrt{\frac{1}{2} e_{ij} e_{ij}}, \ a = 25.0 \\ \eta &= \frac{0.015\left(\varepsilon_{vc} + \varepsilon_{v,ini}\right)}{\varepsilon_{v,\lim}} \end{aligned} \tag{10}$$

The multi-yield surface plasticity model has two main advantages. First, it can easily simulate the shear cyclic responses by means of the simplified algorithm with rather few material constants. Second, the path-dependency of soil can be represented only by the plastic strains (e_{mpij}) of all constituent components. As the multi-component scheme has similaritieswith the contact density model of crack shear transfer [15] and the multi-directional crack modeling of reinforced concrete [7], higher stability of computing soil-RC structural interaction is made possible.

The multi-yield surface plasticity model has been used to simulate both the static and seismic behaviors of nonlinear soil-structure systems [15 and 16]. Regarding the liquefiable soil-RC interaction, the applicability of the models used in this paper was examined and verified by Maki *et al.*[8]. Fig. 3 shows the computed pure shear stress-strain relation and the corresponding effective mean stress of the soilskeleton for different relative densities under the perfect undrained state.

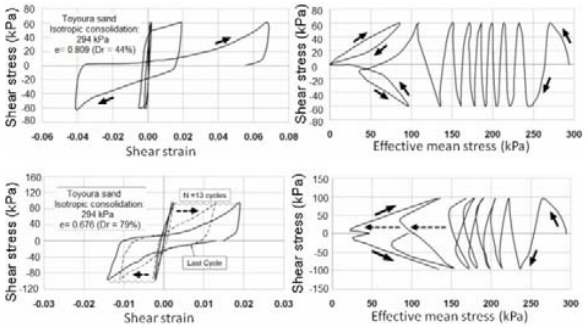

(a) Shear stress strain relation of Toyoura sand under undrainedcondition (after Towhata 2008[3])Upper: loose sand, Lower: densely compacted sand

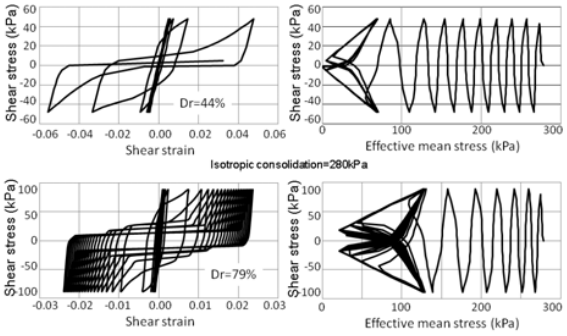

(b) Computed shear stress strain relation under undrained condition Upper: loose sand, Lower: densely compacted sand

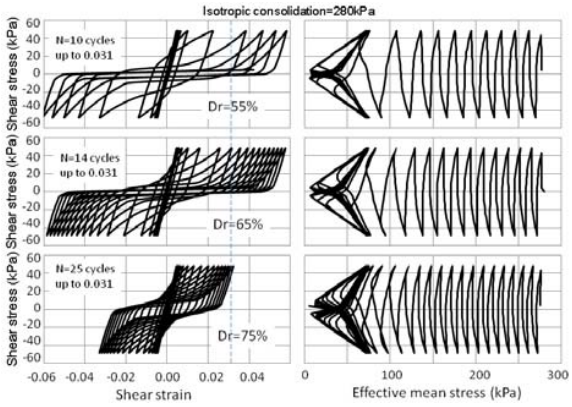

(c) Computed shear stress strain relation under undrained condition Sensitivity analysis in regard to the relative density: The same initial stiffness assumed

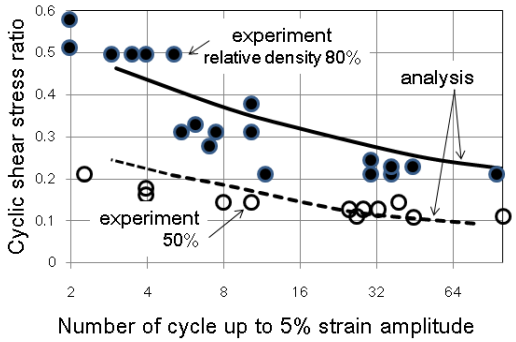

(d) Computed cyclic undrained triaxial strength in comparison with experiments [17]

Fig. 3 Series of Confinement dependent soil model under undrained cyclic shear loading

III. Large Scale Shaking Table Test

A large-scale test for group piles with a sheet pile quay wall subjected to liquefaction-induced large ground deformation was performed by Motamed *et al.*(2009) [5]. This experiment was executed in March 2006 at National Research Institute for Earth Science and Disaster Prevention (NIED), Hyogo Earthquake Engineering Research Center, Japan. Liquefactioninduced lateral spreading was achieved and soil moved laterally about 1.1m behind the sheet pile. Lateral soil displacement was measured by the inclinometers. Bending strain records were able to quantitatively show the damage profile to the piles, i.e., yielding at the top and buckling at the middle height. The experiment was simulated by using the constitutive models in section II. The analytical results shows similar deformation mode of soil-superstructure system and the failure profile along the piles as well.

A. Experimental Setup of the Large Scale Shaking Table Test

Fig. 4 shows schematic plane and cross-sectional views of the model whichconsisted of a 2x3 pile groups located behind a sheet pile quay wall. The model was constructed in a huge rigid box with the dimension of 16m x 5m x 4m. Albany silica sand was used as a liquefiable soil with relative density of 60 %, initial shear stiffness about 20-50 MPa, and the specific gravity 2.63. The steel sheet pile wall used in the experiment was LSP-2 type. Six hollow steel piles with outer diameter 152.4 mm and thickness 2 mm were used to support 22 ton weight of the super structure. The large scale model was shaken under two-dimensional input motion, i.e., the horizontal and vertical components. The acceleration time histories were a scaled-dawn (80%) version of the records obtained at Japan Railway Takatori station during the 1995 Kobe Earthquake (Fig. 5). The maximum amplitude of the horizontal component was scaled as 0.6g and maximum amplitude of the vertical component was scaled as 0.23g. The vertical and horizontal acceleration records, which range from 5 to 20 sec, are underlined in this simulation, since the motion was terminated beyond this range as shown in Fig. 5.

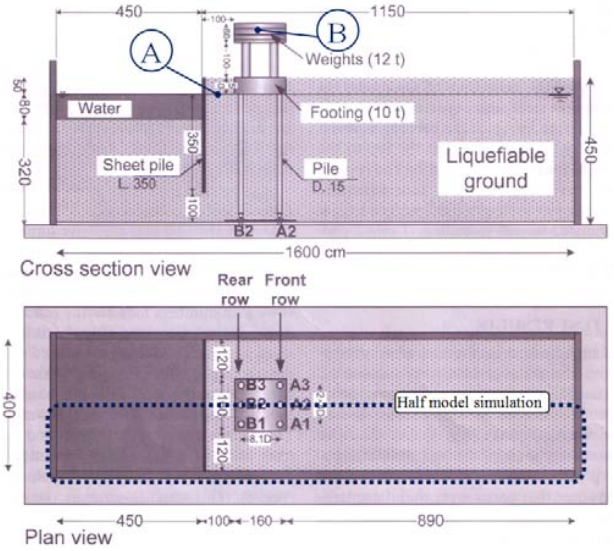

Fig. 4 Cross section and plane views of 2x3 pile group and sheet pile quay wall-large scale test in E-Defense (unit: cm) [5]

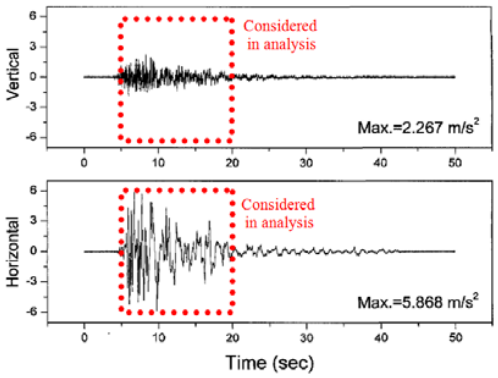

Fig. 5 Acceleration time histories of input motion [5]

B. Analytical Model of Large Scale Shaking Table Test

The steel pilesare simulated by Timoshenko frame element (fiber cross section [7]). Soil box, steel sheet pile wall, and superstructure were modeled as elastic solid elements. Soil was modeled as graded 9 layers of soft soil with equivalent mechanical properties. As a result of full symmetry, longitudinal half of the model was simulated to accelerate the analysis and reduce the time consuming as shown in Fig. 6.

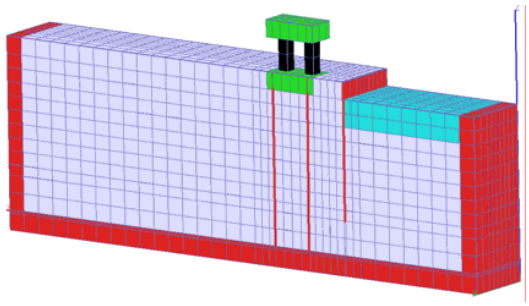

Fig. 6 3D finite element half-model of large scale experiment

C. Analytical and Experimental Results of Large Scale Shaking Table Test

Failure Mode of Piles

Bending strain along the piles was recorded during the experiment by pasted pairs of strain gauges in the direction of liquefied soil lateral flow. The bending strain records and the analytical simulation model show large negative bending strain which develops at the piles heads, while large positive bending strain was attained at the middle height of the piles (Fig. 7). These observations were consistent with plastic deformation in the steel piles. Since the fiber cross section frame element was used to simulate the steel piles and the curvature profile could be computed, the bending strain was directly calculated from the computed curvature as described in Eq. 11. Numerically and experimentally, it isclearly shown that a sudden increase in the strain at shallow depth (pile head) occurred as a result of flexure failure (footing sudden tilting) at the time of 10.2 seconds (PGA time) as shown in Fig. 8.

$$Bending\ strain\ (\varepsilon_b) = \Psi * D/2 \qquad (11)$$

whereΨ is the computed curvature at pile head, and D is the steel pile outer diameter.

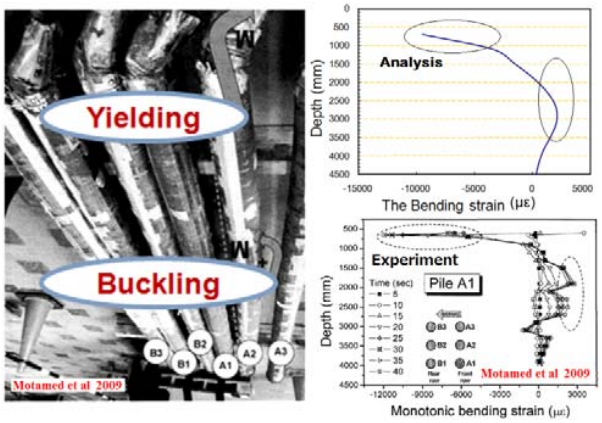

Fig. 7 Analytical and experimental Pile mode of failure behind quay wall during liquefaction of soil

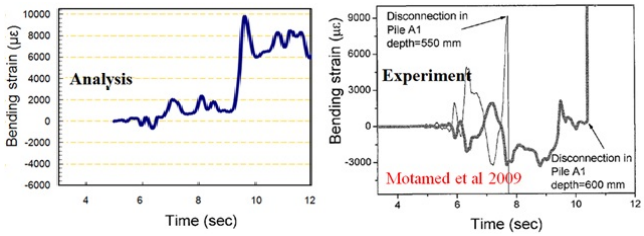

Fig. 8 Analytical and experimental bending strain at pile head

Lateral Movement of Soil and Superstructure

During the dynamic shaking, large lateral deformation took place to the extensively liquefied soil and superstructure toward the water side as shown in Fig. 9. It should be noticed that the flexural failure at the pile head started around the time of 10.2 sec, which may cause a sudden tilting toward the soil side. Thesoil lateral deformation behind the quay wall was measured by using the wiretype displacement transducer and for the superstructure by using the non-contact type laser displacement transducer. The soil lateral displacement behind the quay wall during shaking in the analytical model is picked out at point A illustrated in Fig. 4 and is plotted with experimental lateral displacement(residual soil displacement profile in time)as shown in Fig. 10. The superstructure lateral displacement during shaking in the analytical model is picked up at point B as illustrated in Fig. 4 and is plotted with the experimentally measuredlateral displacement as indicated in Fig. 11. Finally, the lateral displacements of both soil behind quay wall, and superstructure are fairly reproduced, and a qualitatively reasonable profile of pile damages is shown in Fig. 10 and Fig. 11 of the experimental and analytical results.

As the material functions in section II are made based on the Toyoura sand specimens, the simulation is not consistent with Albany sand used in this study. Then, the detailed quantitative discussion is hardly made.

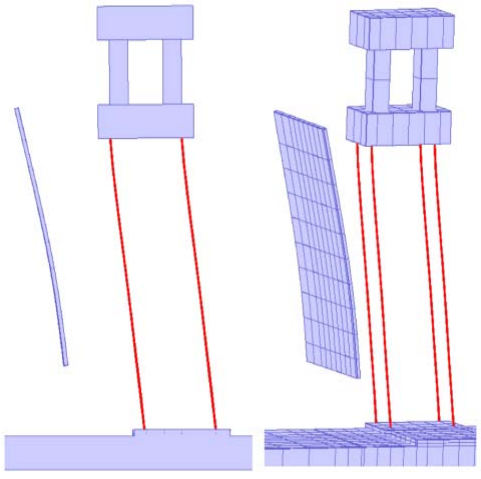

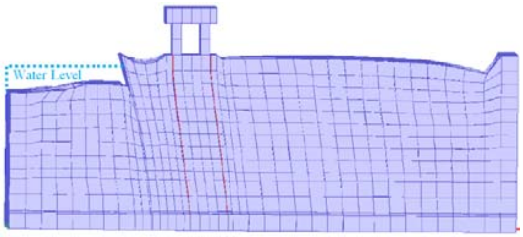

Fig. 9 The lateral deformation of the analytical model

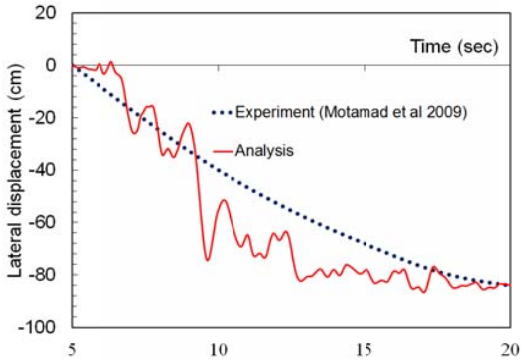

Fig. 10 Analytical and experimental soil lateral movement behind Quay wall at point A

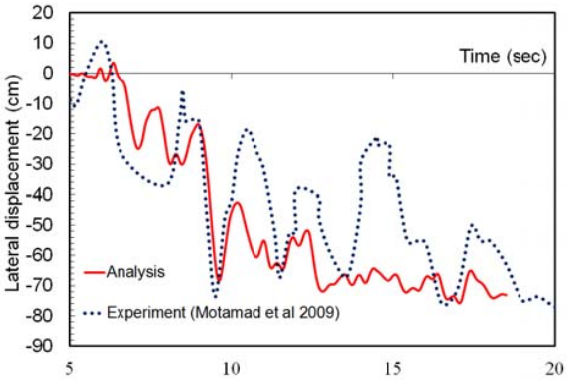

Fig. 11 Analytical and experimental superstructure lateral displacement at point B

IV. Small Scale Shaking Table Test

A. Experimental Setup of Small Scale Shaking Table Test

Maki *et al*(2004)[6] conducted a number of shaking table tests to evaluate the post-yield damages of RC piles embedded in the liquefied soil foundation (Fig. 12a). Four cases were studied as shown in Fig. 12b, i.e.,Case A and Case B for a single pile, while case C and Case D for group piles.

For Case A and Case C, two different layers of sandy soil were placed in the shear container. Soil A and Soil B were made of Hamaoka sand, but with different relative density.

Soil A (Dr =40%) is much looser than the compacted Soil B (Dr =80%), which means soil A is easier to be liquefied. Besides, pure soil cases without pile were also studied as a benchmark cases.

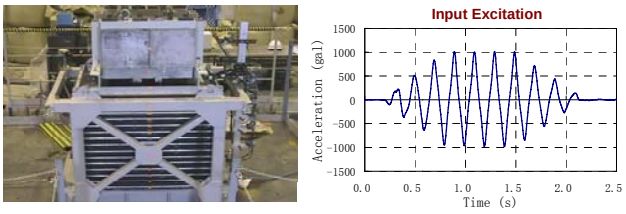

(a) Experiment setup and input excitation

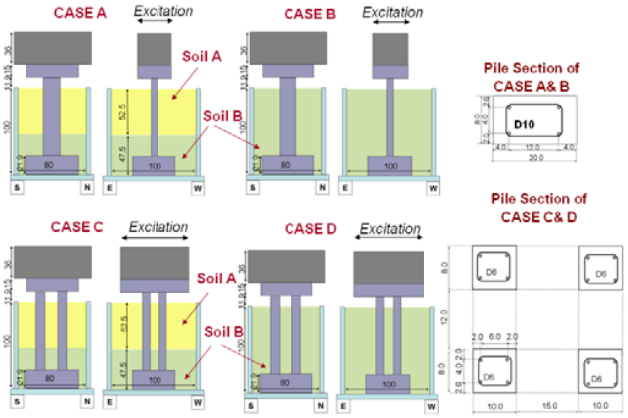

(b) Experimental studied cases and the pile section

Fig. 12 Small scale shaking table test properties [6]

B. Analytical Model of Small Scale Shaking Table Test

Analyses with the modeling in section II have been carried out to simulate all the cases. Undrained condition is applied in Case A and Case C, and 3D quadrilateral solid elements are usedfor both soil and RC piles as the size of pile section is comparatively large according to the shaking table as shown in Fig. 13. Elastic truss elements are placed only along the horizontal direction at outside surface of the finite elements to represent the confining effect of the laminar shear box used in the dynamic test.

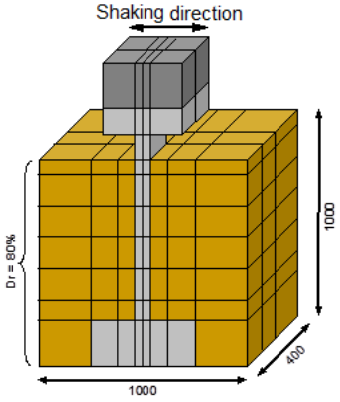

Fig. 13 3D finite element model of small scale experiment

C. Analytical and Experimental Results of Small Scale Shaking Table Test

Soil layers in Case A and Case C were kept in the saturated condition and liquefied due to the shakings in the test. Fig. 14

illustrates the pore water pressure rises inside the upper loose layer at different depths. It can be said that this layer easily liquefies soon after shaking starts, which coincides with the observations made during the experiment. Besides, plastic hinges were formed at the bottom end of the piles, i.e., reinforcing bars yielded and concrete cracks developed along the piles in the experiments as shown in Fig. 15. Although Case B and Case D were conducted in dry conditions, there are still cracking and yielding of reinforcement bars throughout the piles as shown in Fig. 15. Thus, both of the nonlinearity of liquefied soil and RC piles can be checked and examined in these experiments.

Fig. 16 demonstrates the analytical and experimentally measured displacement and the accelogramsat the soil surface in the case where no RC pile is placed. Then, the modeling of soil which is originally specified for Toyoura sand is thought not so far from the mechanistic character of Toyoura sand used in this case. Furthermore, Fig. 17 indicates the calculated displacementat the soil surface and the top of the RC piles, and its comparison with experimental data in Cases A-D. It can be said that the analysis may capture the responses as a whole. Fig. 18 shows the deflections and strain profile along piles for Case A and Case B at a peak deformation. It can be understood that cracking of concrete and yield of steel bars took place along the piles as observed in the experiments.

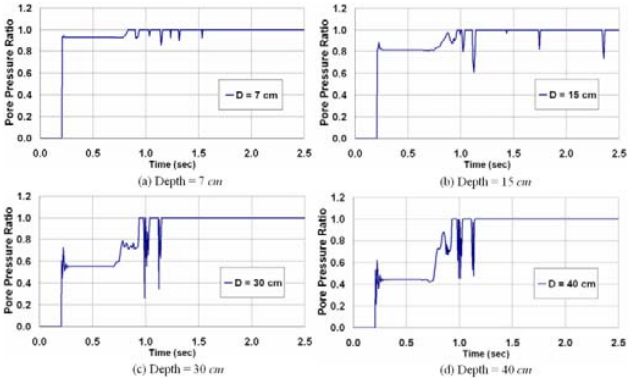

Fig. 14 Pore water pressure development inside loose soil at different depths; No RC column

Fig. 15 Crack patterns of RC piles in different cases of experiment [6]

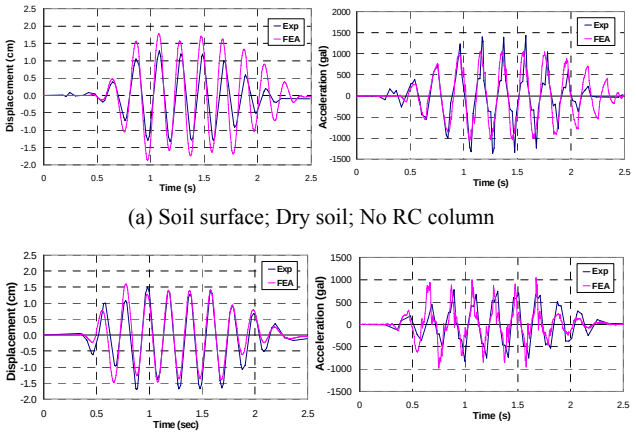

(a) Soil surface; Dry soil; No RC column

(b) Soil surface; Liquefied soil; No RC column

Fig. 16 Comparison of calculated displacement and acceleration response with experimental data

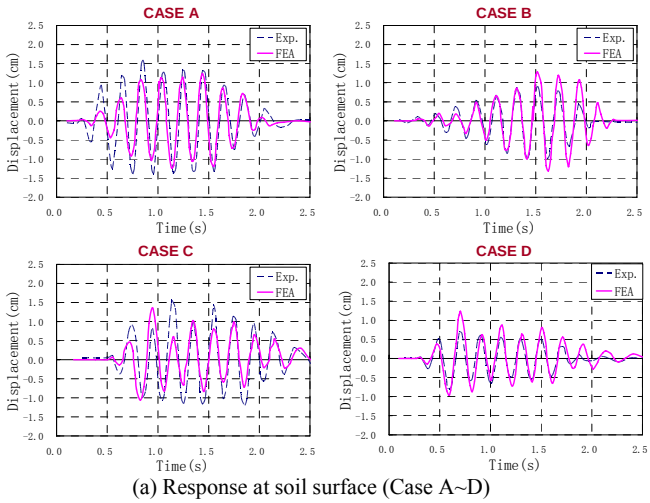

(a) Response at soil surface (Case A~D)

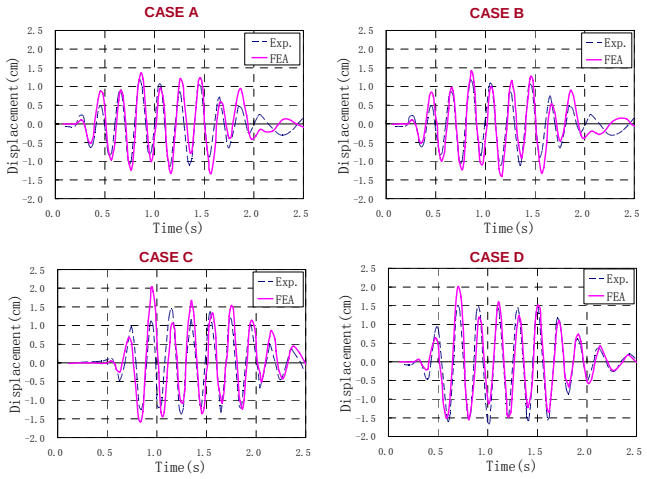

(b) Response at top of RC model structure (Case A~D)

Fig. 17 Comparison of calculated displacement response with experimental data

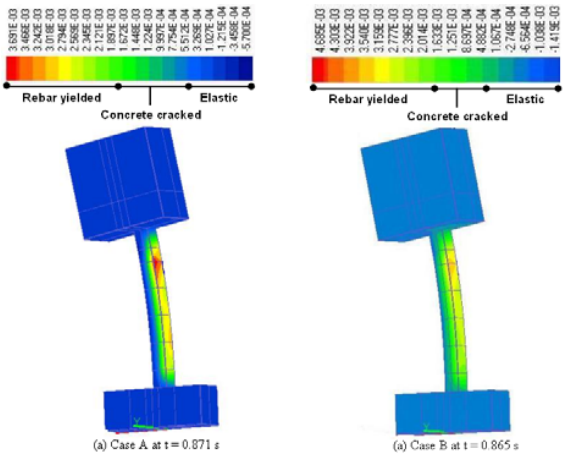

Fig. 18 Deflections (magnified 10 times) and strain profile of RC piles in the small experiment

V. Conclusion

1) Soil liquefaction brings about the reduced shear stiffness, which may relax the local section forces of piles around the softened foundation. On the others hand, globally magnified is the overall deformation of liquefied foundation, which may lead to damages of piles especially around the point of stiffness change like support, joints and interfacesbetween soil layers of different mechanics. This trade-off observed in dynamic soil-pile tests can be simulated by considering nonlinear path-dependency of soil, steel and reinforced concrete.
2) For damage evaluation after the earthquake, post-failure modeling for cracking, yielding and local buckling is needed. These local events of material failure are verified to be linked with space-averaged strain of cracked concrete elements. With this, overall damage profile of steel and RC piles can be presented, and quantitatively consistent with the experimental facts.
3) The material characteristic functions used in the analysis were simply identified by the test for Toyoura sand. Then, the simulation of the test with other sands does not exactly match the experiments but the inelastic nonlinear interaction beyond the failure of piles can be qualitatively captured. It is confirmed that the overall soil deformation may govern the damage profiles of piles inside the liquefied foundation.

References

[1] Hamada, M.(1992). "Large ground deformations and their effects on lifelines: 1964Niigata earthquake. Case studies of liquefaction and lifelines performance during past earthquakes," Technical Report NCEER-92-0001, Volume 1, Japanese Case Studies, National Centre for Earthquake Engineering Research. Buffalo, NY.
[2] Wilson, D. W. (1998) "Soil-pile-superstructure interaction in liquefying sand and soft clay," PhD thesis, University of California, Davis, CA.
[3] Towhata, I. (2008). "Geotechnical Earthquake Engineering," Springer, Germany.
[4] Mohammed, A. M. Y., Okhovat, M. R., and Maekawa, K. (2012). "Damage Evolution of Underground Structural Reinforced Concrete: -Small-Scale Static-Loading Experiments," International Journal of World Academy of Science, Engineering and Technology, 6,696-703.
[5] Motamed, R.,Towhata ,I., Honda, T.,Yasuda, S., Tabata, K.,Nakazawa, H. (2009). "Behavior ofpile group behind a sheet pile quay wall subjected to liquefaction-induced large ground deformation observed in shaking test in E-Defense project,"Soils and foundations, 49(3), 459-475.
[6] Maki, T., Maekawa, K., Nakarai, K. and Hirano, K. (2004). "Nonlinear response of RC pile foundations in liquefying soil," Japan Geotechnical Society.
[7] Maekawa, K., Pimanmas, A. and Okamura, H. (2003). "Nonlinear Mechanics of Reinforced Concrete," Spon Press, London.
[8] Maki, T., Maekawa, K., and Mutsuyoshi, H. (2005). "RC pile-soil interaction analysis using a 3D-finite element method with fiber theory-based beam elements," Earthquake Engineering and Structural Dynamics, 99, 1-26.
[9] Tuladhar, R., Maki, T., and Mutsuyoshi, H. (2008). "Cyclic behavior of laterally loaded concrete piles embedded into cohesive soil," Earthquake Engineering and Structural Dynamics, 37, 43–59.
[10] Okhovat, M. R., and Maekawa, K.(2009) " Damage control of underground RC structures subjected to service and seismic loads," PhD thesis, University of Tokyo.
[11] Kato, B. (1979). "Mechanical properties of steel under load cycles idealizing seismic action," CEB Bulletin D'Information, 131, 7-27.
[12] Towhata, I. and Ishihara, K. (1985) "Modeling soil behaviors under principal stress axes rotation," 5th Int. Conf. on Numerical Method in Geomechanics, Nagoya, 523-30.
[13] Masing, G.(1926)"Eigenspannungen and VerfestigungBeim Messing," Proc. of Second International Congress of Applied Mechanics, 332, Zurich.
[14] Maekawa, K. and An, X. (2000). "Shear failure and ductility of RC columns after yielding of main reinforcement," Engineering Fracture Mechanics, 65, 335-368.
[15] Li, B., Maekawa, K. and Okamura, H. (1989). "Contact density model for stress transfer across crack in concrete," Journal of Faculty of Engineering, University of Tokyo (B), 40(1), 9-52.
[16] Nam, S. H., Songa, H. W., Byuna, K. J., Maekawa, K. (2006)" Seismic analysis of undergroundreinforced concrete structures consideringelasto-plastic interface element with thickness,"Engineering Structures, 28, 1122-1131.
[17] Toki, S., Tatsuoka, F., Miura, S., Yoshimi, Y., Yasuda, S. and Makihara, Y. (1986). "Cyclic undrained triaxial strength of sand by cooperative test program," Soils and Foundations, 26(3), 117-128.